

## Physical and Mechanical Properties, Effect of Thermal Annealing in Vacuum and in Air on Nanograin Sizes in Hard and Superhard Coatings Zr-Ti-Si-N

**Abstract.** Zr-Ti-Si-N coating had high thermal stability of phase composition and remained structure state under thermal annealing temperatures reached 1180°C in vacuum and 830°C in air. Effect of isochronous annealing on phase composition, structure, and stress state of Zr-Ti-Si-N ion-plasma deposited coatings (nanocomposite coatings) was reported. Below 1000°C annealing temperature in vacuum, changing of phase composition is determined by appearing of siliconitride crystallites ( $B-Si_3N_4$ ) with hexagonal crystalline lattice and by formation of  $ZrO_2$  oxide crystallites. Formation of the latter did not result in decay of solid solution (ZrTi)N but increased in it a specific content of Ti-component. Vacuum annealing increased sizes of solid solution nanocrystallites from (12 to 15) and as-deposited coatings to 25 nm after annealing temperature reached 1180°C. One could also find macro- and microrelaxations, which were accompanied by formation of deformation defects, which values reached 15.5 vol.%. Under 530°C annealing in vacuum or in air, nanocomposite coating hardness increased. When Ti and Si concentration increased and three phases nc-ZrN, (Zr, Ti)N-nc, and  $\alpha-Si_3N_4$  were formed, average hardness increased to (40,8±4) GPa. Annealing to 500°C increased hardness and demonstrated lower spread in values  $H=(48±6)$  GPa and  $E=(456±78)$  GPa.

**Streszczenie.** Powłoki Zr-Ti-Si-N posiadają wysoką stabilność termiczną składu fazowego i zachowują stan strukturalny w temperaturach wygrzewania poniżej 1180°C w próżni i 830°C w powietrzu. Opisany został wpływ wygrzewania izochronicznego na skład fazowy, budowę i stan naprężeń powłok Zr-Ti-Si-N nanoszonych jonowo (powłok nanokompozytowych). W próżni, w temperaturach wygrzewania poniżej 1000°C, zmiany składu fazowego są określone poprzez pojawianie się krystalitów azotku krzemu ( $B-Si_3N_4$ ) o heksagonalnej sieci krystalicznej oraz przez tworzenie krystalitów tlenku  $ZrO_2$ . Tworzenie tych ostatnich nie powodowało rozpadu roztworu stałego (ZrTi)N, jednakże zwiększyło w nim zawartość składnika Ti. Wygrzewania próżniowe zwiększyło rozmiary nanokrystalitów roztworu od 12 do 15 i wytworzonej powłoki do 25 nm po osiągnięciu temperatury wygrzewania 1180°C. Możliwe było także odnalezienie makro- i mikrorelaksacji, którym towarzyszyło tworzenie defektów o wartości osiagającej 15,5 obj.%. Poniżej temperatury wygrzewania 530°C w próżni lub w powietrzu twardość powłoki nanokompozytowej wzrastała. Przy wzroście koncentracji Ti oraz Si powstają trzy fazy nc-ZrN, (Zr, Ti)N-nc oraz  $\alpha-Si_3N_4$  a średnia twardość wzrastała do 40,8±4 GPa. Wygrzewanie do 500°C zwiększyło twardość i wykazało niższy rozrzut wartości  $H=(48±6)$  GPa oraz  $E=(456±78)$  GPa. (Fizyczne i mechaniczne właściwości, wpływ wygrzewania w próżni i w powietrzu na nanorozmiarowe ziarna w twardych i supertwardych powłokach Zr-Ti-Si-N).

**Key words:** annealing, nanocomposite, Zr-Ti-Si-N, hardness, nanograin, superhard.

**Słowa kluczowe:** wygrzewanie, nanokompozyty, Zr-Ti-Si-N, twardość, nanoziarno, supertwardy.

### 1. Introduction

Recently, nanocomposite coatings of new generation composed of at least two phases with nanocrystalline and/or amorphous structures are of great interest [1]. As is known, there are two groups of hard and superhard nanocomposites with nc-MeN/hard phase and nc-MeN/soft phase [2-5]. Moreover, bicrystalline phases and/or phases with different crystallographic grain orientations of the same material are distinguished in nanocrystalline and/or amorphous phases. Experimental data of a number of authors demonstrated that Zr-Si-N system was composed of two phases ZrN and (Si, Zr)N [6]. It is possible to assume that Ti addition to this system, would allow one to obtain several phases: nc-ZrN/ $\alpha-Si_3N_4$  and nc-TiSi<sub>2</sub> with definite Si and N concentrations. As it is known from works [7,8], properties of solid  $\alpha-Si_3N_4$ /McN strongly depend on phase composition and thermal stability of individual phases composing the total coating. It was demonstrated that Zr-Si-N films with  $ZrN_x$  ( $x = 0.8$ ) composition were thermally stable till 1130°C. Those of  $ZrN_x$  ( $x = 1.2$ ) composition, i.e. having higher Zr concentration, like ( $\alpha-Si_3N_4$ /MeN)  $Si_3N_4 + ZrN_x$  ( $x = 1.2$ ), were crystallized under higher temperature of 1530°C ( $x = N/Zr$  in  $ZrN_x$  phase). However, when  $Si_3N_4$  phase was amorphous and took more than 50 vol.% of the coating, hardness ranged from 20 to 40 GPa, i.e. did not transit superhardness limit of 40 GPa [5, 8, 9].

We should like to note works [6], in which the authors studied structure stability and mechanical properties of Ti-Zr-N films deposited by vacuum-arc source (Cathodic Arc Vapor Deposition – CAVD) under various plasma densities from metallic cathodes Ti and Zr.

Also we should like to note theoretical works [3, 4], which studied electron structure, stability, decohesion mechanism, shear of interfaces in superhard and heterostructures nc-TmN/ $\alpha-Si_3N_4$ .

Therefore, the purpose of this work was to study formation of superhard coatings on Zr-Ti-Si-N base and their properties including thermal stability.

### 2. Experimental

Coatings were fabricated using vacuum-arc deposition from unit-cast, Zr, Zr-Si, and Zr-Ti-Si targets. Films were deposited in nitrogen atmosphere. Deposition was carried out using standard vacuum-arc and HF discharge methods. Bias potential was applied to substrate from HF generator, which produced impulses of convergent oscillations with  $\leq 1$  MHz frequency, every impulse duration being 60  $\mu$ s, their repetition frequency – about 10 kHz. Due to HF diode effect, value of negative autobias potential occurring in substrate increased from 2 to 3 kV at the beginning of impulse (after start of discharger operation). Coatings of 2 to 3.5  $\mu$ m thickness were deposited to steel substrates (of 20 and 30 mm diameter and 3 to 5 mm thickness). Deposition was performed without additional substrate heating. Zr-Ti-Si-N coatings were deposited to polycrystalline steel (St.3 – 0.3 wt.% C, Fe the rest). Molecular nitrogen was employed as a reaction gas (Table 1).

$I_a$  is cathode current in A;  $P_N$  is pressure of atomic nitrogen in Pa units;  $U_{RF}$  is bias voltage of HF discharge;  $U$  is bias voltage under conditions of vacuum-arc discharge. Annealing was performed in air medium, in a furnace SNOL 8.2/1100 (Kharkov, Ukraine), under temperature  $T = 300^\circ C$ ,  $500^\circ C$ , and  $800^\circ C$ , and in a vacuum furnace SNVE-1.3, under  $5 \times 10^{-4}$  Pa pressure, and  $T = 300^\circ C$ ,  $500^\circ C$ ,  $800^\circ C$ ,

and 1180°C. Studies of phase compositions and structures were performed using X-ray diffraction devices DRON-3M, under filtered emission Cu-K $\alpha$ , using secondary beam of a graphite monochromator. Diffraction spectra were taken point-by-point, with a scanning step  $2\theta = 0.05$  to  $0.1^\circ$ .

Table 1. Physical-technological parameters of deposition

Evaporated materials	Coating	$I_a$ , A	PN, Pa	URF, V	U, V	Notes
Zr	ZrN	110	0.3	-	200	Standard technology
Zr	ZrN	110	0.3	200	-	HF deposition
Zr-Si	(ZrSi)N	110	0.3	200	-	HF deposition
Ti-Zr-Si	(Ti-Zr-Si)N	110	0.3	200	-	HF deposition

To study stressed states of the coatings, we applied X-ray strain and stresses measurements (“ $a - \sin^2 \psi$ ” method) and its modifications, which were used to films with a strong texture of axial type. Element compositions were studied using X-ray fluorescent spectrometer SPRUT (AO UkrRoentgen, Ukraine) with a shoot-through tube employing a silver anode, and under exciting voltage 40kV. Surface morphology, structure, and element compositions were analyzed using a scanning electron microscope (REMMA-103M, Quanta-1000) with microanalysis (EDS-energy disperse X-ray spectroscopy). Additionally, to study element composition and stoichiometry, we used RBS under 1.35MeV  $^4\text{He}^+$  ion energy,  $170^\circ$  scattering angle, and 16keV detector resolution. Studies of mechanical characteristics were realized with the help of nanoindentation under 10nN load of NANOINDENTOR II (MTS System Inc., USA) indentation device with diamond Berkovich pyramid [9].

### 3. Result and discussion

Figure 1 shows energy spectra of ion backscattering measured for steel samples with deposited Zr-Ti-Si-N coatings. Since Zr and Ti concentration was high, these spectra could hardly help to determine Si and N background concentration. Measurements of Si and N concentration using eating away of the RBS spectra gave higher error than for Zr and Ti. But still, Si concentration was not less than 7at.%, while that of N might reach more than 15at.%.

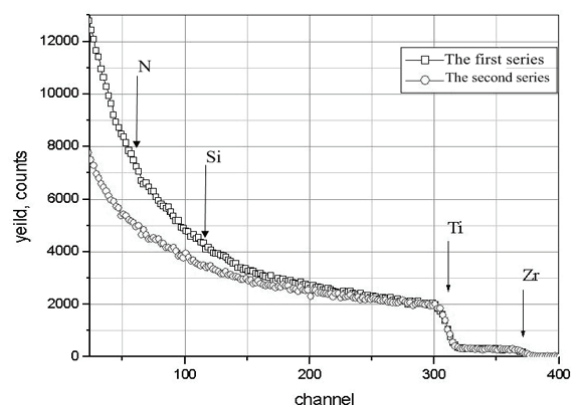


Fig. 1. Energy spectra of Rutherford ion backscattering (RBS) for top thin coating Zr-Ti-Si-N

Analyzing phase composition of Zr-Ti-Si-N films, we found that a basic crystalline component of as-deposition on state was solid solution (Zr, Ti)N based on cubic lattice of structured NaCl. We presents x-ray diffraction curves: a lattice period in non-stressed cross-section ( $a_0$ ), value of macrodeformation  $\epsilon$ , microdeformation  $\langle \epsilon \rangle$ , and concentration of packing defects  $\alpha_{\text{def.pack}}$ . The data were obtained both for samples after coating deposition and for those annealed in vacuum and air under various temperatures.

Crystallites of solid (Zr, Ti)N solution underwent compressing elastic macrostresses occurring in a “film-substrate” system. Compressing stresses, which were present in a plane of growing film, indicated development of compressing deformation in a crystal lattice, which was identified by a shift of diffraction lines in the process of angular surveys (“ $\sin^2 \psi$  – method”) and reached – 2.93% value. With  $E \approx 400\text{GPa}$  characteristic elastic modulus and 0.28 Poisson coefficient, deformation value corresponded to that occurring under action of compressing stresses  $\sigma_c \approx -8.5\text{GPa}$ . We should also note that such high stresses characterize nitride films, which were formed under deposition with high radiation factor, which provided high adhesion to base material and development of compression stresses in the film, which was stiffly bound to the base material due to “atomic peening”- effect.

At substructure level, microdeformation was still high, and amounted 1.4%. With a relatively small average crystallite size ( $L \approx 15\text{nm}$ ), development of such high microdeformation indicated significant contribution of crystallite deformed boundaries.

Phase composition of ion-plasma films under temperature of vacuum annealing lower than  $1000^\circ\text{C}$  remained practically unchanged, corresponding to post as-deposition state. An average crystallite size of solid solution (Zr, Ti)N also remained practically unchanged. Under this temperature range ( $300\text{-}1000^\circ$ ), microdeformation at substructure level typically decreased from 1,4 to 0.8% , which indicated decreasing amount of lattice defects.

Compressing macrodeformation partially relaxed when annealing temperature increased within 25 to  $1000^\circ\text{C}$  range. Practically, it decreased by a factor of three, reaching a value  $\epsilon \approx -1.1\%$  under  $T_{\text{an}} = 1000^\circ\text{C}$ . We should note that  $\epsilon \approx -1\%$ , which was close to that obtained under annealing, was reached in the case of pure, ordered ZrN ion-plasma deposited coatings. A lattice period  $a_0$  defined for non-stressed cross-section (under  $\sin^2 \psi_0 = 0.43$ ) decreased with decreasing annealing temperature. If one would relate such decreased period to ordering of titanium atoms with lower atomic radius, which were built-in into metallic sublattice instead of Zr atoms, then using Vegard’s rule, the decrease from 0.4552nm to 0.4512nm corresponded to 8.5at.% to 19.5at.% increase of titanium atom content.

Shift of diffraction lines to various directions corresponding to planes taken at  $\theta - 2\theta$  (according to Bregg-Brentano scheme) seems to be explained by packing defects, which are present in metallic fcc-sublattice. Concentration of packing defects may be evaluated by comparison of shifting (222) and non-shifting (333) peak positions [10]. After condensation, average packing defect concentration in a lattice of (Zr, Ti)N solid solution was 5.7%. As a result of annealing, packing defect concentration increased and reached 15.5% under  $T_{\text{an}} = 800^\circ\text{C}$ .

Qualitative changing of phase composition was observed in films under vacuum annealing at  $T_{\text{an}} > 1000^\circ\text{C}$ .

Appearance of zirconium and titanium oxides was related to oxidation relaxation under coating surface interaction with oxygen atoms coming from residual vacuum atmosphere under annealing. Under annealing

temperatures below 1000°C, coatings phase composition remained practically unchanged (Fig.2 ). One could note only changed width of diffraction lines and their shift to higher diffraction angles. The latter characterizes relaxation of compressing stresses in coatings. Changed diffraction lines were related to increased crystalline sizes (in general) and decreased micro-deformation.

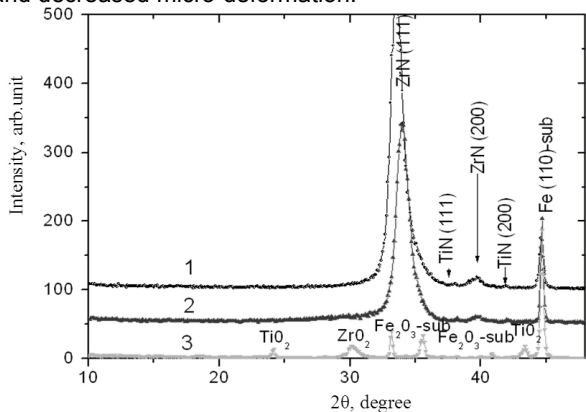


Fig.2. XRD diffraction patterns for Zr-Ti-Si target in 0.3Pa nitrogen atmosphere (vacuum-arc source with HF discharge): 1 - for initial (as-received) samples; 2 - for annealed at 500°C (30min in vacuum); 3 - for annealed at 800°C (30min in vacuum)

Figure 3 shows the film cross-section, which demonstrates that in the course of deposition, no cracks were found, that indicated good quality of the coating. These results indicated that amount of N is essentially high, and this allowed it to participate in formation of nitrides with Zr, Ti, or (Zr, Ti)N solid solution. Si concentration was low, however, results reported by Veprek et al. [3, 4] indicated Si concentration as high as 6 to 7at.%, which was enough to form siliconitride phases.

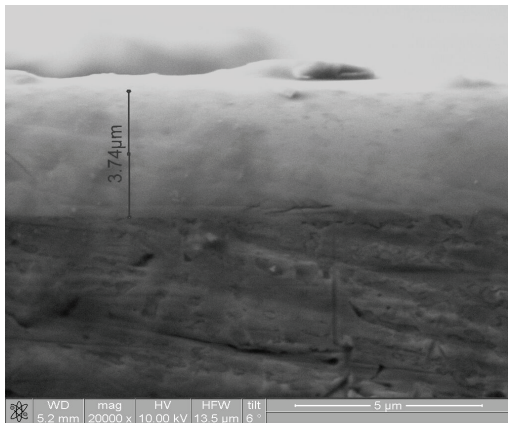


Fig.3. Cross-section of hard coating Zr-Ti-Si-N (high concentration of Si and N)

Changes occurred under macrodeformation of crystallites of basic film phase – (Zr, Ti)N solid solution. Compressing deformation of crystallite lattices increased, which seemed to be related to additional new crystalline components, which appeared in film material: oxides and siliconitrides. In the lattice itself, a period decreased corresponding to increased Ti concentration. Ordered atoms in metallic (Zr/Ti) sublattice of solid solution increased from 8.5 to 21at.%. In this temperature range, crystallite size increased from 15 to 25nm, crystallite lattice microdeformation increasing non-essentially up 0.5 to 0.8%[10,11]. summarizes substructure characteristics of (Zr, Ti)N solid solution crystallites.

Figure 4, shows XRD-diffraction patterns, and lower (b), a histogram of volume phases for nano-structured Zr-Si-N

coating with 10 to 12nm grain sizes for *nc-ZrH* phase (where *nc* is a nano-structured phase). These data demonstrate 17% volume fraction of quasi-amorphous  $\alpha$ - $\text{Si}_3\text{N}_4$  phase, 54% of nano-composite nano-structured phases, and the rest was  $\alpha$ -Fe from samples substrates.

When annealing temperature came close to 550°C to 600°C range[12], the process of spinodal segregation was over, i.e. all nano-grains were totally surrounded by an interlayer of several  $\alpha$ - $\text{Si}_3\text{N}_4$  nano-layers (quasi-amorphous phase).

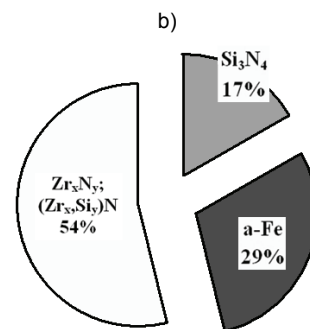
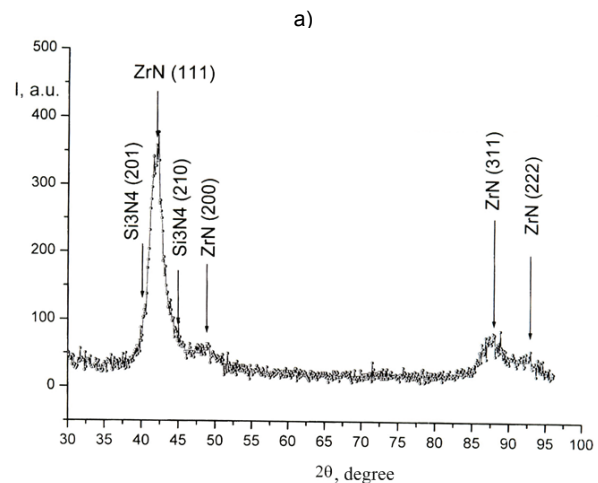


Fig.4. (a) A fragment of diffraction patterns for Zr-Si-N coating deposited by vacuum-arc method with HF stimulation ( $\text{Fe-K}_\alpha$  radiation); (b) Histogram of phase ratio for nanocomposite coatings Zr-Si-N

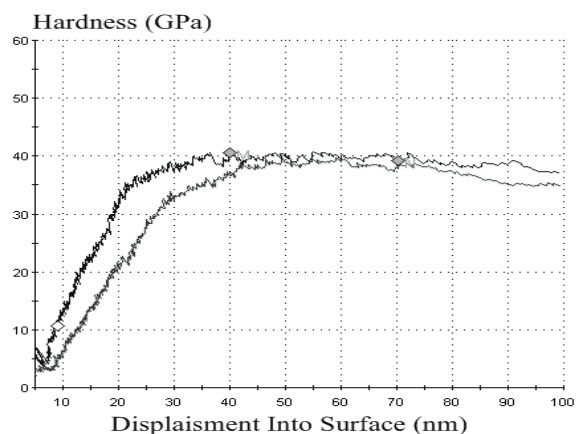


Fig.5. Load on sample vs displacement into surface

In initial state, after deposition, those samples (second series), which phase composition included three phases (Zr,Ti)N-nc, ZrN-nc, and  $\alpha$ - $\text{Si}_3\text{N}_4$ , hardness was  $H = 40,6 \pm 4\text{GPa}$ ;  $E = 392 \pm 26\text{GPa}$  (Fig.5). 500°C annealing increased

H and E and decreased spread in hardness values, for example,  $H = 48 \pm 6$  GPa and  $E = (456 \pm 78)$  GPa.

In such a way, hardness, which was increased in the process of annealing, seems to be related to incomplete spinodal phase segregation at grain boundaries resulting from deposition of Zr-Ti-Si-N-(nanocomposite).

Annealing stimulated spinodal phase segregation [3, 4], forming more stable modulated film structures with alternating in volume concentration of phase components (ZrN; (Zr,Ti)N;  $Si_3N_4$ ).

#### 4. Conclusion

In such a way, decreased concentration of active oxygen atoms coming from annealing atmosphere increased stability of film phase composition from 500 to 1000°C. Changing crystalline phase composition was determined by crystallization of siliconitrides and formation of  $\beta - Si_3N_4$  crystallites with hexagonal lattice, as well as low  $ZrO_2$  concentration formed in the film surface.

The relaxation was accompanied by formation of deformation packing defects in a metallic sublattice of (Zr, Ti)N solid solution. This can be revealed by X-ray scanning, which demonstrated shift and broadening of diffraction peaks. Highest content of packing defects indicated shift of most closely packed planes in a fcc-sublattice (111) with respect to each other [1, 4, 8, 11] and became pronounced under vacuum annealing at  $T_{an} = 800$  to 1100°C reaching 15.5vol.%.

When Ti and Si concentration increased (second series) and three phases nc-Zr-N, (Zr, Ti)N-nc, and  $\alpha-Si_3N_4$  were formed, average hardness increased to  $40,8 \pm 4$  GPa. After annealing (a dark dotted curve) at 500°C in vacuum, coating nanohardness reached  $H = 55.3$  GPa.

In Zr-Ti-Si-N coatings, increased Ti concentration, formation of three phases- (Zr, Ti)N-nc-57vol.%, TiN-nc-35vol.%, and  $\alpha - Si_3N_4 \geq 7.5$  vol.%, as well as changes of grain size, which decreased to (6 to 8)nm in (Zr, Ti)N and (10 to 12) in TiN in comparison with first series resulted in increased nanohardness and decreased difference in hardness values. Annealing in vacuum below 500°C finished the process of spinodal segregation at grain boundaries and interfaces. Annealing stimulated segregation processes and formed stable modulated coating structure [1, 4, 8, 13].

The work was funded by the program "Nanosystems, Nanomaterials and Nanocoatings. New Principles in Nanomaterial Manufacturing by Ion, Plasma and Electron Beams" NAS of Ukraine.

#### REFERENCES

[1] Pogrebnjak A.D., Shpak A.P., Azarenkov N.A., Beresnev V.M., Structures and Properties of Hard and

- Superhard Nanocomposite Coatings, *Usp. Phys.*, 179 (2009), 35-64
- [2] Musil J., Zeman P., Hard  $a-Si_3N_4/MeN_x$  nanocomposite coatings with high thermal stability and high oxidation resistance, *Solid. State. Phenome*, 127, (2007), 31-36
- [3] Zhang R.F., Argon A.S., Veprek S., Electronic structure, stability, and mechanism of the decohesion and shear of interfaces in superhard nanocomposites and heterostructures, *Phys. Rev.*, 79 (2009), art. no. 245426
- [4] Veprek S., Veprek-Heijman M.G.J., Karvankova P., Prochazka J., Different approaches to superhard coatings and nanocomposites, *Thin Solid Films*, 476, 1 (2005), 1-29
- [5] Musil J., Dohnal P., Zeman P., Physical properties and high-temperature oxidation resistance of sputtered  $Si_3N_4$  MoNx nanocomposite coatings, *Vac. Sci. Technology*, 23 (4), (2005), 1568-1575
- [6] Uglov V.V., Anishcik V.M., Zlotski S.V., Abadias G., Dub S.N., Structural and mechanical stability upon annealing of arc-deposited Ti-Zr-N coatings, *Surf. and Coat. Tech.*, 202 (11), (2008), 2394-2398
- [7] Azarenkov N.A., Beresnev V.M., Pogrebnjak A.D. Structure and Properties of Coatings and Modified Layers of Materials. – Kharkov: KhNU, 565, (2007)
- [8] Gavaleiro A., De Hosson J.T., Nanostructure Coating, 340, (2006)
- [9] Musil J., Physical and Mechanical Properties of Hard Nanocomposite Films Prepared by Reactive Magnetron Sputtering. Ch. 10/Eds. A. Cavaleiro, J.Th.M. De Hosson. – Kluwer Academic/Plenum Publishers. (N.-Y. USA), (2005)
- [10] Vishniakov Ja.D., Moscow: Metallurgija, 480.(1975)
- [11] Sobol, O.V., Pogrebnjak, A.D., Beresnev, V.M. Effect of the Preparation Conditions on the Phase Composition, Structure, and Mechanical Characteristics of Vacuum Arc Zr-Ti-Si-N Coatings The Physics of Metals and Metallography Vol. 112 №2 2011: pp.188-195.
- [12] Pogrebnjak A.D., Danilionok M.M, Uglov V.V., Erdybaeva N.K., Kirik G.V., Dub S.N., Rusakov V.S., Shpylenko A.P., Zukovski P.V., Tuleushev Y.Zh., Nanocomposite protective coatings based on Ti-N-Cr/Ni-Cr-B-Si-Fe, their structure and properties, *Vacuum*, 83 (2009), 235-239
- [13] Pogrebnjak A.D., Ponomarev A.G., Shpak A.P., Kunitskii Yu.A., Application of micro-nanoprobes for the analysis of small-size 3D materials, nanosystems, and nanoobjects, *Usp. Phys. Nauk*, 182 (3) (2012), 287-321

**Authors:** prof. Aleksander D. Pogrebnjak, Ahmad M. Mahmood, Artem A. Demianenko, Vyacheslav S. Baidak, Andrii P. Shpylenko, Sumy State University, Sumy Institute for Surface Modification., 2, R-Korsakov Str., 40007 Sumy, Ukraine, E-mail: [alexp@i.ua](mailto:alexp@i.ua)  
prof. Vyacheslav M. Beresnev, Vladimir V. Grudnitskii, Kharkov National University, 4, Svobody Sq. Str., 61022, Kharkov, Ukraine;  
prof. Pawel Zhukowski, Department of Electrical Devices and H.V. Technology, 38a Nadbystrzycka Str., 20-618, Lublin, Poland, E-mail: [pawel@elektron.pol.lublin.pl](mailto:pawel@elektron.pol.lublin.pl).